ELSEVIER

Nuclear Physics A631 (1998) 242c–261c

NUCLEAR PHYSICS A

Results of Recent Bremsstrahlung Measurements on Few-Body Systems at KVI

N. Kalantar-Nayestanaki[a]

[a]Rijksuniversiteit Groningen, KVI,
Zernikelaan 25, 9747 AA Groningen, The Netherlands

A series of bremsstrahlung measurements have been performed with the superconducting cyclotron, AGOR, at KVI. These measurements, on the proton-proton and proton-deuteron systems, aim to investigate the nucleon-nucleon interaction as the nucleons go off their mass shell. Cross sections and analyzing powers have been measured for all possible exit channels of both systems with an incident proton energy of 190 MeV, which is below the particle-production threshold. Preliminary results of the real-photon as well as virtual-photon production are presented and compared to theoretical predictions.

1. INTRODUCTION

Nucleon-nucleon bremsstrahlung is the most fundamental reaction used in studying the off-shell behavior of the nucleon-nucleon interaction as it involves the strong interaction between two nucleons, and the well-known electromagnetic interaction. In addition, the cross section for nucleon-nucleon bremsstrahlung is the basis of all calculations which deal with photon production in heavy-ion collisions. These calculations rely heavily on theoretical predictions of the nucleon-nucleon bremsstrahlung process, which resort to approximations such as the soft-photon approximation that, to leading order, contains no off-shell information. This process was looked at for the first time in detail for an incident energy of 250 MeV in a theoretical paper by Ashkin and Marshak [1]. In this paper, differential cross sections were derived for the proton-proton bremsstrahlung. In 1958, Low proved that in a series expansion, in photon momentum, of the differential cross section, the first two terms can be exactly calculated in terms of elastic amplitude for the same system [2]. Another approach for the low-energy calculations was made by Feshbach and Yennie [3].

A serious look at the off-shell behaviour of different potential models was taken in 1963 by Sobel and Cromer [4] when it was also known that experiments could be performed to be compared to the predictions. The potentials used in their calculations gave bremsstrahlung cross sections which differed by a factor 2 to 3 from each other. However, the parameters of these potentials were obtained by fitting to a relatively small set of data available at the time. Calculations also included the effect of non-coplanarity where the two outgoing proton vectors do not form a plane with the incoming proton vector [5]. As the process was better understood, other ingredients such as double scattering [6] and relativistic spin corrections [7] were added in the calculations. At the same time, more

PII S0375-9474(98)00026-8

refined nucleon-nucleon potentials were becoming available [8].

On the experimental grounds, one has a different situation. The huge elastic background has always hampered the efforts to perform a high-luminosity measurement because of the problems with the singles count rate. This, in turn, will make it difficult to get a clean bremsstrahlung signal out of measurements. Most of the first generation experiments performed in the 60's measured the outgoing protons at larger angles (larger than 20°) to avoid interference with beam and beam-related background at smaller angles. Gottschalk et al. [9] measured for the first time the non-coplanar events and studied the behaviour of the cross section as a function of non-coplanarity. Rothe and coworkers [10] measured the direction of the outgoing photons as well as the outgoing protons, thereby increasing the number of parameters with which the measurement is overdetermined. They also measured, for the first time, analyzing powers of the process. However, the polarized-beam intensity for this measurement was rather low ($\approx 2 \times 10^7$ protons/sec). All these measurements used liquid hydrogen targets with rather thick windows.

Recently, the study of off-shell effects by nucleon-nucleon bremsstrahlung below the particle-production threshold has been receiving increasing attention both theoretically and experimentally. The reason for this is the success of modern potential-model calculations on the one hand and the advent of high-precision detection systems on the other [11–19].

Polarized-proton beams and high-flux neutron beams have also delivered a boost to the experimental efforts. Recent cross-section and analyzing-power data from TRIUMF [12] clearly show the need for the inclusion of off-shell effects in the calculations. With even higher accuracies achievable nowadays, one can hope to study, in detail, the properties of the off-shell nucleon as it propagates in an intermediate state as well as the non-nucleonic degrees of freedom (such as Δ–excitation) which can even admix at energies below the pion-production threshold. In this contribution, after a brief review of nucleon-nucleon bremsstrahlung (in the proton-proton and the proton-deuteron systems) in section 2, the experimental setup used in the KVI measurements is sketched in section 3. The analysis is outlined in section 4 and the preliminary results are discussed in 5. A summary with some outlook is presented in 6.

2. NUCLEON-NUCLEON BREMSSTRAHLUNG AND THE KVI EXPERIMENT

In Figure 1, various amplitudes used in the calculations of the bremsstrahlung process are depicted. Figure 1a shows the external-bremsstrahlung (single-scattering) amplitude, where the photon can be emitted before or after the strong interaction, and in Figure 1b the internal-bremsstrahlung (double-scattering) amplitude is represented. The meson-exchange current (MEC) and the delta contributions are schematically shown in Figure 1c along with relativistic contributions. For proton-proton bremsstrahlung, MEC is absent in the leading order. For proton-neutron bremsstrahlung, on the contrary, MEC contributions are the largest for higher photon energies. Dipole and quadrupole structures of the electric contributions for $pn\gamma$ and $pp\gamma$, respectively, are dominant in the photon angular distributions at lower photon energies. Calculations show [15], however, that the off-shell effect is enhanced for higher photon energies where the magnetic contribution becomes

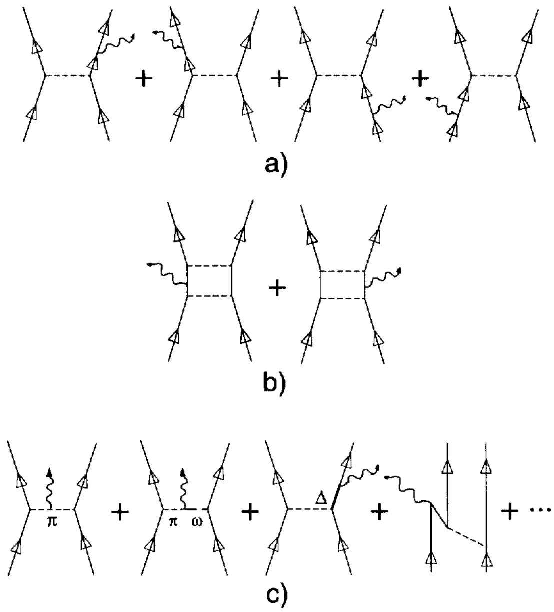

Figure 1. *The amplitudes for the different terms in the bremsstrahlung process: a) external bremsstrahlung (single scattering), b) internal bremsstrahlung (double scattering), and c) meson-exchange-currents, delta and $N\bar{N}$ contributions.*

stronger relative to the electric contribution. It is worth noting that, for some kinematics, the contribution of $pp\gamma$ can be as much as 20% of that of the $pn\gamma$ and should not be ignored in the nucleus-nucleus reaction-mechanism studies. Finally, note that in studying the high-energy photon emission in the $NN\gamma$ process, one has to detect the outgoing nucleons at small angles.

Even though the subject of bremsstrahlung is a rather old one, it has only been possible in the last decade to obtain data for proton scattering to small angles with high enough accuracies to make a sensible comparison with potential-model calculations. For the first time, a high-intensity polarized-proton beam was used in an experiment at TRIUMF [12] where cross sections and analyzing powers for proton-proton bremsstrahlung were measured for incident proton energies just below the pion-production threshold and for small outgoing proton angles. In this experiment, a coplanar geometry was chosen in which the two outgoing protons and the photon lie in the same plane. The calculations [12] done for the TRIUMF experiment and also those done by Herrmann and Nakayama [20] show that the shapes of both cross-section and analyzing-power data can only be reproduced if the off-shell effects are included in the calculation. From these and other calculations, it also became clear that with the typical experimental accuracies attained, no distinction can be made between different modern potential models. Modern potential-model calculations which take into account the effect of double scattering and relativistic spin correction generally agree with each other to a few percent [11]. It should be noted that the TRIUMF data were normalized by a factor 2/3 by the authors of the paper [12]. Without this normalization, the cross-section data overshoots the calculations by about 50%. This normalization problem should, however, be resolved by experiments with higher accuracies.

It has been shown that the nucleon form factor is modified as it goes off the mass shell [21–23]. This modification will change the magnetic form factor of the NNγ, leaving the electric one unchanged because of charge conservation. Recent calculations show that polarization observables such as spin-correlation coefficients are especially sensitive to these effects in the case of proton-proton bremsstrahlung where the magnetic coupling plays a more dominant role at higher photon energies [24,25]. However, these coefficients are much more difficult to measure experimentally.

The Δ-isobar contribution in the intermediate state and the effect of Meson Exchange Currents (MEC) have been studied in detail by several people [19,26,27]. In the proton-proton system, the contribution of the intermediate Δ is larger than in the proton-neutron system due to isospin factors. Even though all these contributions are relatively small, precise measurements and selected kinematics should distinguish between models with or without them.

The situation on the proton-neutron bremsstrahlung is quite different. Generally speaking, the neutron beams lack the high quality and/or intensity required for precise measurements [28,29]. Because of this, the cross sections presented in the literature have been rather inclusive. An ongoing experiment at Los Alamos Neutron Science Center will produce, for the first time, exclusive data, though limited in statistical accuracies, in which the outgoing particles are detected [30]. In the past, the proton-deuteron system was chosen for the investigation of the proton-neutron bremsstrahlung. The complication with this choice is, of course, the Fermi motion of the nucleons in the deuteron. The recent experiments performed [31,32] have also been inclusive, i.e. only the outgoing photon has been detected leaving no access to the details of the reaction. There exist no good calculations for this process. Any calculation attempting to describe the inclusive result should treat all the possible outgoing channels of this reaction properly. These include:

1. $p + d \longrightarrow {}^3\mathrm{He} + \gamma$
2. $p + d \longrightarrow p + d + \gamma$
3. $p + d \longrightarrow p + n + p_{spec} + \gamma$
4. $p + d \longrightarrow p + p + n_{spec} + \gamma$

The first channel, the radiative capture, has the highest photon energy. The center-of-mass energy available in this reaction is high enough ($E_\gamma^{CM} \approx 127$ MeV for our case) to distinguish it from the other channels. However, this high energy also makes the calculations very difficult as one not only has to include all the multipolarities in the electromagnetic operator but also the exact nature of the deuteron and ^{3}He wave functions should be well known in calculating the overlap integral. Due to correlations, the S component of the ^{3}He$\rightarrow p$+d vertex goes through a zero in the energy region which includes our energy, thus enhancing the contribution of the D-wave admixtures. Therefore, the knowledge of the relative behaviour of S and D waves is essential in the calculations. The D component of the vertex is primarily determined by the D waves in ^{3}He [33].

The second channel represents the "coherent" bremsstrahlung from the deuteron. This reaction is like the nucleon-nucleon bremsstrahlung except that any calculation dealing with it should include all the intermediate channels (the deuteron has a binding energy of 2.2 MeV). If one takes the simple picture that the deuteron is a loosely bound object and that the incoming proton interacts primarily with a nucleon, then this channel can provide a clear signal for the final-state interaction effects.

The other two channels are very similar in nature. One is the bremsstrahlung as a result of proton-neutron interaction while the other proton is the spectator (aside from final- and initial-state interactions) and the other is the bremsstrahlung in the proton-proton interaction with the neutron being the spectator. The Fermi motion of the nucleon results in production of higher energy photons as compared with the free nucleon-nucleon bremsstrahlung. The calculation done by Nakayama [34] in which the free neutron-proton bremsstrahlung cross section is "folded" with the momentum distribution function of the nucleons in the deuteron fails to explain the data. This is not surprising in view of the fact that the other channels discussed above have not been taken into account in this calculation. In fact, even the procedure with which the free nucleon-nucleon bremsstrahlung is folded with the momentum distribution of the neutron is not a trivial matter [35]. It is clear that with the free proton-proton data (from the proton-proton system), and the quasi-free proton-proton data (channel 4 above) of the proton-deuteron system, one can test the folding procedure and the initial- and final-state effects. If these are well understood, one can then use channel 3 to unfold the free proton-neutron bremsstrahlung process from the $p+d$ system.

Aside from the real-photon production, one can also study the virtual-photon production in the same systems. This latter process involves an extra electromagnetic vertex, thereby reducing the cross section by at least a factor α, the fine-structure constant, as compared with the former one. However, the whole territory of virtual-photon production on light systems in intermediate-energy regime is virgin. There are two new aspects of this process that are of interest. First, the cross section can be studied as a function of the non-zero photon invariant mass. Secondly, aside from the transverse response function present in the case of the real-photon production, one can in principle study other response functions such as the longitudinal response function and the interference terms in the nuclear currents that are relevant in the reaction. Experiments which involve measurements of all the outgoing particles will provide a check on theoretical calculations such as the recent ones which primarily concentrate on the Soft-Photon Approximation (SPA) [36]. Finally, using polarized protons and looking at the ϕ-angular distribution of the reaction cross section will provide polarization-transfer coefficients. These observables have never been measured before.

The KVI bremsstrahlung program with AGOR on few-body systems, set out to study and measure the cross sections and analyzing powers of all the above-mentioned reactions in a series of measurements specifically tuned for nucleon-nucleon bremsstrahlung. The measurements started with the proton-proton system and extended to the proton-deuteron system. One of the goals of the experiment is to measure high-precision cross sections to settle the question of the absolute normalization raised by the TRIUMF data [12]. In addition to coplanar geometry, non-coplanar geometries have been measured for a large number of angle combinations. Angular coverage of protons is from 6° to 26° and photons were measured from $\approx 57°$ to $\approx 176°$. All the measurements are exclusive in the sense that all the outgoing particles, where possible, were measured. Besides, all the measurements were carried out using polarized protons.

3. EXPERIMENTAL APPARATUS

To probe matrix elements involving intermediate states that are far off the mass shell, we need to measure high energy photons. This in turn restricts the detection of the protons to small laboratory angles. However, at small angles one is limited by the quality of the beam and the very high rate of proton-proton elastic scattering (for the forward detector considered here, this rate is about 1.0×10^7 counts/s). The high-quality polarized proton beam at AGOR overcomes the first limitation. The problem of high rates was dealt with by employing a highly segmented detection system. The polarized protons of 190 MeV were delivered by the superconducting cyclotron, AGOR, with typical polarization of 50% to 70%. Due to the high elastic rates in the detection system, the beam current was kept under 10 nA. The beam, going through our detection system, was stopped about 10 meters further downstream in a very well-shielded Faraday cup. In the following subsections, various parts of the detection systems and the target are outlined.

3.1. SALAD

To detect the outgoing hadrons at forward angles, the Small-Angle Large-Acceptance Detector, SALAD, was designed and built. This detector which was built for a precise measurement of the absolute cross sections and analyzing powers is schematically shown in Figure 2. It is a detection system with almost cylindrical symmetry which measures particles between 6° and 19° for the whole azimuthal angular range and proton energies of up to 130 MeV with a resolution of about 5%. The upper limit of the range of the polar angles increases to about 26° for a smaller region of the azimuthal angles. The large solid angle (about 500 msr) is mandated by the very small cross sections of the nucleon-nucleon bremsstrahlung process. To allow the beam free passage, our detector was designed with a central hole.

To determine the coordinates of the charged particles, we used two wire chambers (MWPC) the first of which with three planes (x, y, and 45°) to overcome ambiguities in multi-prong events. The second chamber has two planes (x and y). The wire spacing in these chambers is 2 mm. However, to reduce the number of read-out channels, every two adjacent wires go through one amplifier-discriminator channel. The anode-cathode spacing is 4 mm. The angular resolution obtained with these chambers is better than 0.5°. A high detection efficiency was observed even at high rates of more than 100 kHz on each wire [37].

Plastic scintillators are used to measure the energy of the particles: a thick layer, consisting of 24 elements, detecting the particles originating from bremsstrahlung events is backed by a thin layer, consisting of 26 elements, vetoing protons of higher energies coming from elastic events and punching through the thick layer.

For the $pp\gamma$ experiment, the trigger of SALAD for the bremsstrahlung event is as

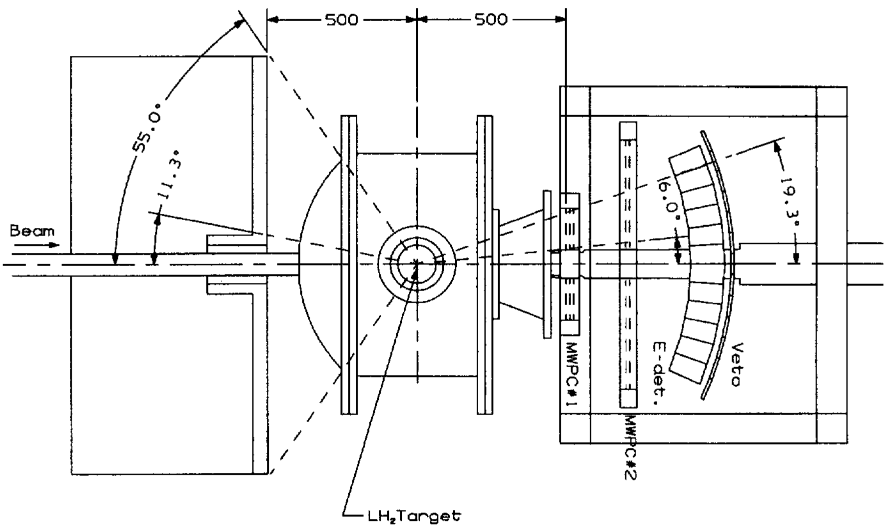

Figure 2. *A schematic top view of SALAD. Half of the scintillators are read out from the top and the other half from the bottom. TAPS was placed around the target mostly at angles larger than* 57° *(here, the "supercluster" configuration is depicted.). The beam pipe goes through the center of all detectors.*

follows: when a minimum of two of the energy scintillators of SALAD have fired, a trigger box, designed at KVI, will look to see whether any veto detector has fired [38]. A valid SALAD trigger is when the number of energy detectors minus the number of veto detectors is at least 2, $N_E - N_V \geq 2$. However, as was mentioned earlier, because of the chosen geometry, SALAD will be flooded with unwanted events stemming from elastic proton-proton scattering. Due to hadronic interaction, it can easily be seen that the number of double elastics within a certain gate is so large that the detection of the photons in time coincidence is mandatory. The photon detection is further used to reduce the background as the measured photon parameters are used in the analysis.

3.2. TAPS

For the measurement of the position and the energy of the photons, we used the Two-Arm Photon Spectrometer, TAPS [39], which was placed in two different geometries in our experiment, the "supercluster" and the "block" geometries. In order to keep the almost complete cylindrical symmetry, we used the "supercluster" configuration of TAPS. In this configuration, all the crystals were placed in a hexagonal frame surrounding the beam pipe upstream from the target covering an angular range of 125° – 170°. This cylindrical symmetry is essential in adding up measured counts for the whole range of the azimuthal angle for high statistics.

In order to look at the angular distribution of the reaction, the crystals were redistributed in 6 rectangular frames, each containing 64 crystals. These were positioned on both sides of the beam line around the target covering an angular range of 57° – 176°. This geometry is referred to as "block" geometry. The vertical acceptance of a block is 42°. In both geometries, TAPS covered more than 20% of the full 4π solid angle.

It should be noted that the "supercluster" configuration lacks the thin plastic scintillators, usually referred to as charged-particle veto counters placed in front of the crystals in the "block" configuration. However, since the "supercluster" was placed at backward angles, the contribution from charged particles to the background should not be very large. The thin plastic scintillators were used in the "block" geometry in order to identify the e^+ and e^- particles in the virtual bremsstrahlung measurements [40].

With the "supercluster" geometry, both coplanar and non-coplanar events were measured simultaneously with high statistics as the counts for the whole azimuthal-angle range can be added. For the "block" geometry, this is no longer true thus limiting the statistical accuracy of the measurements.

3.3. Target

We used a liquid hydrogen/deuterium target for these measurements [41]. A 6 mm thick disk with a diameter of 20 mm was filled with the desired liquid. The operational temperature and pressure were somewhat above the triple point of the substance in question. This way, the exerted pressure on the window would be minimal enabling us to use very thin windows. For the dimensions of our target, we use 4 μm-thick Aramid (from Toray, Japan) windows. This is the first time that such a thin window of synthetic material has been used in a beam of protons. These windows were used for extended periods of running like 2 to 3 weeks at a time. The beam current was typically 6 nA for the proton-proton system and 1 nA for the proton-deuteron system.

4. ANALYSIS

The data were stored on DLT tapes on line and later filtered once to make a first selection on the raw data. The analysis of the virtual-bremsstrahlung measurements is outlined in [40]. Here, the analysis of the real-bremsstrahlung measurements is represented.

Five measured angles, namely the polar and azimuthal angles, θ and ϕ, of the two outgoing particles (protons and deuterons in first instance) and the polar angle of the photon, θ_γ, and the incident proton energy were used to inspect the event. If there was no violation of kinematics, the event was used further in the analysis. For the accepted events, other variables such as the energy of the outgoing proton or deuteron and the energy and the azimuthal angle, ϕ_γ, of the photon were consequently reconstructed.

Since we measure all the variables of the experiment (except the energy and position of the neutron in the first phase of the experiment), we have an overdetermined kinematics which allows us to cut more background and have a better confidence in the quality of the data.

The p+p and the p+d systems should be separately treated. The p+p system is rather straight forward. The final state is a 3-body final state and measuring 9 variables in the experiment leaves us with 4 overdetermined variables which could be used for further reduction of the background. As was mentioned earlier, the p+d system ends up with 4 final states. The first channel (the radiative-capture channel) is a 2-body final state. Detecting the photon is already enough to reconstruct the event. The detection of the recoil ^{3}He will give extra variables for redundancy check. However, the radiative-capture data presented in this paper are obtained from the singles measurement. The second channel (the "coherent" bremsstrahlung on the p+d system) is a 3-body final state and, as far as the analysis is concerned, is essentially identical to the p+p system. The only difficulty is the particle identification which we have to extract from the analysis itself. The third and the fourth channels in the p+d system (the "quasi-free" bremsstrahlung) are the most difficult to deal with. The position detection of the neutron was not possible in the first phase of the experiments as we wanted the high-rate capability of SALAD for both TAPS geometries in the proton-proton bremsstrahlung measurements. Therefore, the only channel we can sensibly look at in the "supercluster" geometry of TAPS is the 4-body final state with two protons and the photon detected. Assuming that the neutron was the spectator, one can go ahead and reconstruct the event just as in the free p+p case. However, even with this assumption, Fermi motion will result in the broadening of all envelopes containing momenta, etc.

The power of reconstruction in cutting the background is shown in Figure 3. In the top part, all the events in the coincidence window (started by the protons or deuterons and 80 ns wide) are shown. The prompt photon peak is in the middle of the window. When these events are checked for energy and momentum conservation, a vast majority of them do not survive and the ones that do will almost always stay in the prompt peak; see the bottom panel of the figure. The redundancy of variables for the events has not been used in the procedure to obtain the spectrum at the bottom of the figure. That will further reduce the background.

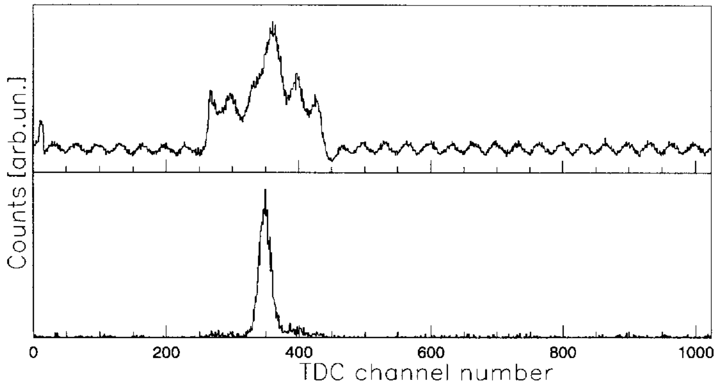

Figure 3. *The time distribution of events. Top part of the figure is the event time for all events registered as good* $pp\gamma$ *candidates while the bottom one shows the events which have satisfied energy and momentum conservation. Each channel is 0.5 ns.*

Figure 4 shows a spectrum which is the result of the reconstruction of the free p+p system. One can observe a band containing the real events, which is much stronger than the surrounding background.

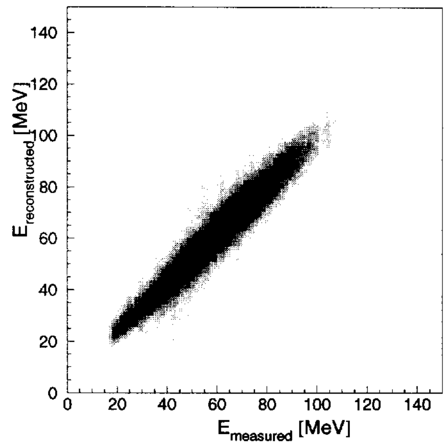

Figure 4. *The reconstructed versus the measured proton energy. Our detector has an energy threshold of about 20 MeV.*

As was mentioned, with the present setup, there is no way of distinguishing the protons from the deuterons resulting from proton-deuteron bremsstrahlung process. In the analysis, one has to check for both possibilities. This is seen in figure 5 where the top-left panel represents the measured versus reconstructed energy of the particles when the mass of the deuteron is assumed. One sees a clear diagonal band corresponding to the deuterons. The other band which is misplaced belongs to protons, then. When the mass of the particle is assumed to be that of the proton, the band which was misplaced ends up on the diagonal and the deuteron band is now misplaced (top-right panel). When one places a cut around these two bands to cut the background, one sees a major improvement in the measured versus reconstructed photon energies; compare the lower-left and lower-right panels of figure 5. The small bands in the top panels come from deuteron break-up events which make it through energy and momentum conservation.

5. PRELIMINARY RESULTS

After all the necessary cuts were made to reduce the background, the surviving events were used for further analysis to obtain cross sections and analyzing powers. In this section, *preliminary* results are presented for the p+p and the p+d systems.

For all the measurements performed on both systems, a fraction of the elastically scattered particles were recorded for normalization and calibration purposes. The elastic-scattering cross sections and analyzing powers for the p+p system are well known from literature. For the p+d system, potential-model calculations for our energy were performed by the Bochum-Cracow group [42]. The measured elastic-scattering cross sections and analyzing powers of both systems were then compared to the calculations. *Preliminary* results show that the pp elastic cross sections, after taking all inefficiencies into account deviate $\approx$ 10% from the calculations when the nominal target thickness and beam

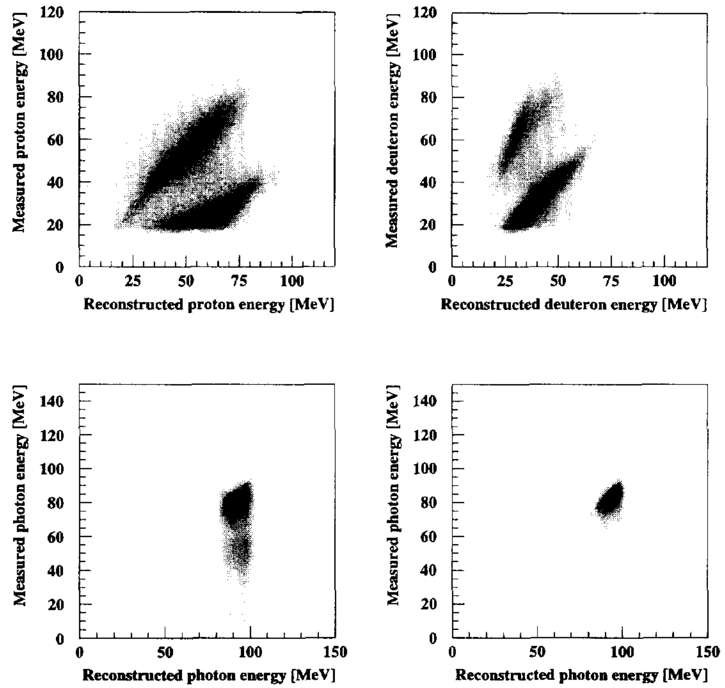

Figure 5. *The measured versus the reconstructed energies for the p+d system. For explanation see text.*

currents are used in the analysis. This data will be used in the final normalization of the data. For the *pd* elastic cross section, the first results deviate between 25% and 35% from the calculations. It should be remarked that *pd* elastic scattering is also less well studied than the *pp* elastic scattering. *Note that no efficiency or absolute normalization factors have been applied to the bremsstrahlung cross sections and analyzing powers presented further on.* The final numbers for the $pp\gamma$ cross sections might move up by about 10%. For the $pd\gamma$ cross sections, this number will be around 25%. Analyzing powers will suffer much less from these normalization and efficiency problems.

5.1. Proton-proton bremsstrahlung

For the *pp* system, measurements were done in two geometries. The first one, the "supercluster" geometry produces high statistics for a limited range of photon polar angles but a complete coverage of the photon azimuthal angle, and the second one, the "block" geometry yields an angular distribution of the bremsstrahlung process with a limited coverage of the photon azimuthal angle. In figure 6, the results of the coplanar cross sections and analyzing powers are presented as a function of the polar angle of one of the protons, while the polar angle of the other proton and the polar angle of the photon are fixed. The coplanar events with the same polar angles have been added in azimuth to increase the statistics in the cross section. The range of non-coplanarity taken in this analysis is 5°. Checks have been made to make sure that the cross-section variations were small up to this angle qualifying these data points as the *coplanar* data.

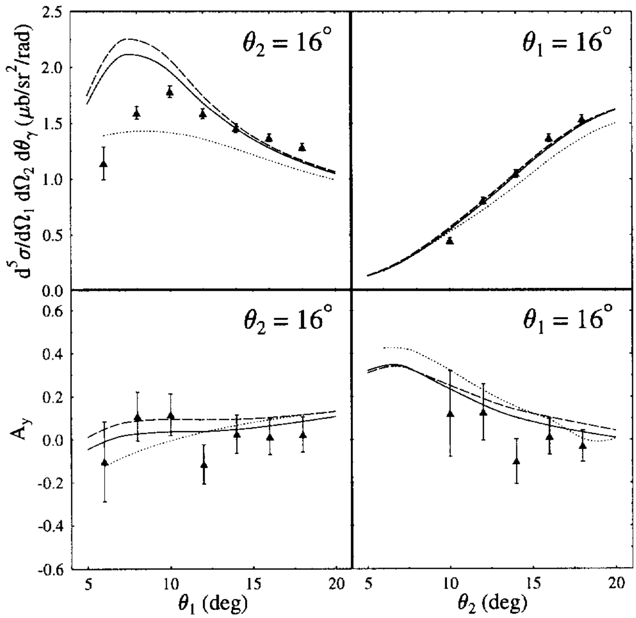

Figure 6. Preliminary *cross sections and analyzing powers as a function of first (left) and second (right) proton polar angles, obtained in the "supercluster" geometry for* $\theta_\gamma = 145°$. *The second (first) proton angle is fixed at* 16°, *respectively. The calculations are SPA (dotted), the "nucleonic calculation" (dashed), and the full calculations including MEC,* $N\bar{N}$ *and the* Δ *as well (solid).*

Two different types of calculations were performed for our kinematics. The first one uses the Soft-Photon Approach (SPA) of Liou, Timmermans and Gibson [43,44]. This calculation is consistent with the low-energy theorem and is relativistic and gauge invariant. The other calculations are done by Martinus, Scholten and Tjon [45]. These calculations include all the possible ingredients shown in figure 1 and treat the nucleons off-shell. To see the higher order effects, a calculation called the "nucleonic calculation" is shown in which only the internal and external bremsstrahlung contributions are considered (figure 1a and 1b), see the dashed curve, and one which includes MEC, $N\bar{N}$ and Δ contributions as well (solid curve). Even though the differences between the data and the calculations are small for the analyzing powers, the cross sections (especially the ones shown in the upper-left panel) deviate from the calculations. The absolute normalization of the data might change by about 10% as mentioned before but this will have no consequence on the shape of the distributions.

In the "block" geometry, we were able to measure the angular distribution of the proton-

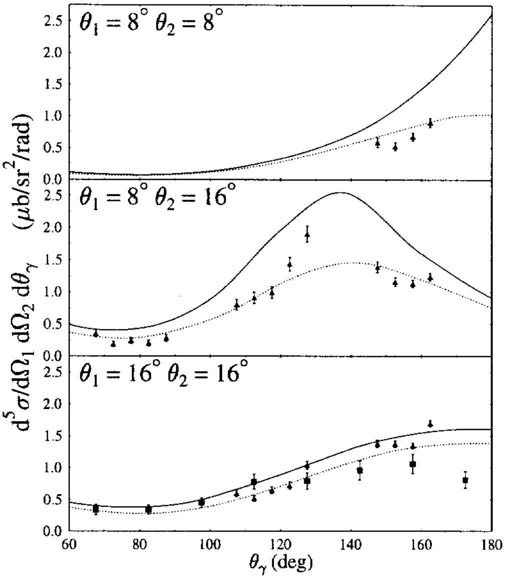

Figure 7. Preliminary *cross sections as a function of* θ_γ *for three different proton-polar-angle combinations indicated on the graphs. The calculations are SPA (dotted) and the "nucleonic" (solid). In the bottom panel, the TRIUMF data with 200 MeV protons [46] are also shown.*

proton bremsstrahlung. However, in this geometry we lost our ability to add the bins of the same azimuthal angle, thereby reducing the accuracy of the measurements compared to the "supercluster" geometry. Nevertheless, we used the total azimuthal acceptance of the blocks to gain more statistics. This procedure is not so simple as the exact acceptance of the block has not been calculated yet with a detailed Monte-Carlo simulation. Because of this, the "block" data were normalized to the "supercluster" data at one common point. The systematical errors should then be looked at more seriously for this geometry. The data are presented in figure 7. Presently, only the cross sections have been analyzed. The presentation of the data is similar to that of the TRIUMF data. Three combinations of θ_1 and θ_2 were chosen. For comparison, the older TRIUMF data at 200 MeV incident proton energy, for which only the outgoing protons were detected, are also shown [46]. The calculations are the SPA (dashed curve) and the "nucleonic" one. As can be seen in the figure, the accuracy of this measurement is inferior to the other geometry. Even though TAPS covered polar angels between 57° and 176°, one sees a much smaller coverage in the figure. This is due to the stopping of low-energy protons on their way to the scintillators of SALAD. With the accuracies (statistical and systematical) obtained for coplanar geometries (non-coplanar geometries have much higher statistics), it is not very easy to make any definitive conclusions about the details of the calculations. One has to inspect the calculations for possibly integrating over some experimental variables to improve the statistics. This is equivalent to comparing the data and the calculations for several neighboring bins simultaneously to have a better understanding of the process.

At very small outgoing proton angles, the bremsstrahlung cross section becomes more dominated by the $^1S_0$ partial wave that has the largest off-shell behaviour of all partial waves with total isospin T=1 [47]. The Coulomb corrections become important for this partial wave. Calculations show [25] that, except for very small proton angles ($\leq 10°$) and for a limited part of the phase space, the Coulomb correction can be neglected. In the case of coplanar geometries, Katsagiannis et al. [48] show that at energies close to our energy, the Coulomb effect is negligible overall.

There are still many more regions of phase space which should be looked at. In particular, non-coplanar geometries (which have a larger phase-space factor thereby higher statistical accuracies) have to be looked at. These are of particular interest for a number of reasons: 1) it will be the first time that such data with high accuracies are measured; 2) one can probe completely different regions of phase space compared to the coplanar geometry; and 3) one obtains more observables (analyzing powers) for these geometries.

Finally, figure 8 shows the cross section as a function of invariant mass of the photon for the virtual proton-proton bremsstrahlung in the "supercluster" geometry. The calculations are similar to other soft-photon approximations [36]. The agreement between the calculations and the data is satisfactory. For more details on the analysis of these data and other spectra, see [40].

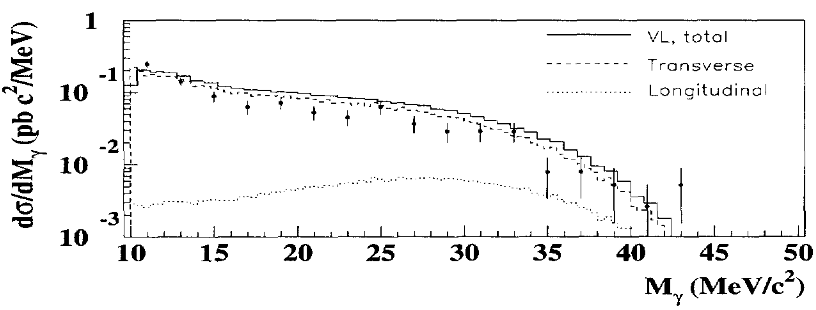

Figure 8. Preliminary *cross section of the virtual proton-proton bremsstrahlung as a function of the invariant mass of the photon. The longitudinal and transverse components of the cross section are separately shown.*

5.2. Proton-deuteron bremsstrahlung

The proton-deuteron bremsstrahlung measurements have only been analyzed in the "supercluster" geometry so far. In this phase of the measurements, neutron detection in SALAD was still not possible. Therefore, the data presented in this section deal with charged-particle detection in SALAD.

In the "supercluster" geometry, the SALAD-TAPS acceptance for coincidence γ–^{3}He detection is rather small. So, in order to have cross sections and analyzing powers for as large an angular range as possible, we decided to analyze the data from the singles photon measurement. This can only be done thanks to the very high photon energy in the radiative-capture process. In fact, after making all the cuts, this is the largest available energy in the detector. Therefore, one has a peak structure which is only hampered at its low-energy side due to overlap with other bremsstrahlung processes. However, it was not difficult to fit the spectra and obtain the contents of the appropriate peak. The *preliminary* results for the cross sections and analyzing powers are presented in figure 9. The IUCF data [49] is also shown for comparison. The agreement between the two data sets is reasonable. Notice that our data has not been corrected for efficiencies, etc. It must also be pointed out that the IUCF data was obtained in a coincidence experiment in which both outgoing particles were detected for background reduction.

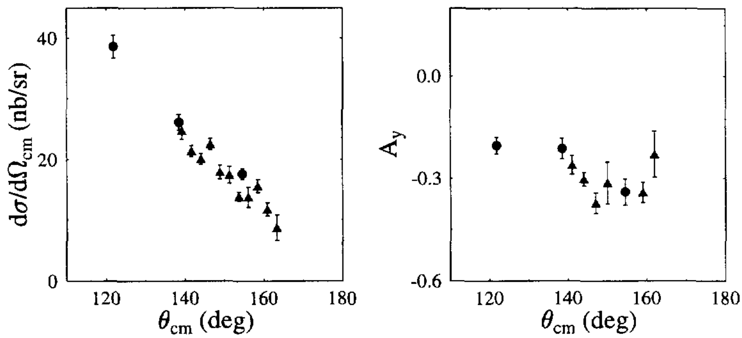

Figure 9. Preliminary *cross-section and analyzing-power data as a function of the photon angle for the radiative-capture process. The filled circles are the IUCF data [49].*

The other channel which was investigated was the 3-body final state or the "coherent" proton-deuteron bremsstrahlung. Except for the particle identification discussed in section 4, the analysis is very similar to the proton-proton bremsstrahlung. The cross sections as a function of θ_γ for four combinations of proton and deuteron polar angles are shown in figure 10. These data, as well as the "quasi-free" data, represent coplanar events. Notice that the photon can be emitted on the proton side but also on the deuteron side giving angles larger than 180°. The calculations which are shown in the figure are Soft-Photon type and classical for the *pn* and *pd* systems, respectively [35]. The information from the elastic *pd* cross sections are not yet included in the *pd* calculations. Therefore, the normalization on the graph is arbitrary. It is remarkable that, as far as the shape is concerned, neither calculation comes close to the data. In the past, one ascribed the emission of the photon primarily to proton-neutron collisions. If this is true, the difference that one observes between the free *pn* calculation and the data must be coming from the Fermi motion of the neutron in the deuteron and the final-state effects fusing the outgoing neutron and proton together. No calculation which attempts to take these effects into account properly has ever been performed. Analyzing powers of the same angle combinations are displayed in figure 11.

Finally, one can assume that the neutrons were spectators in the collision and carried

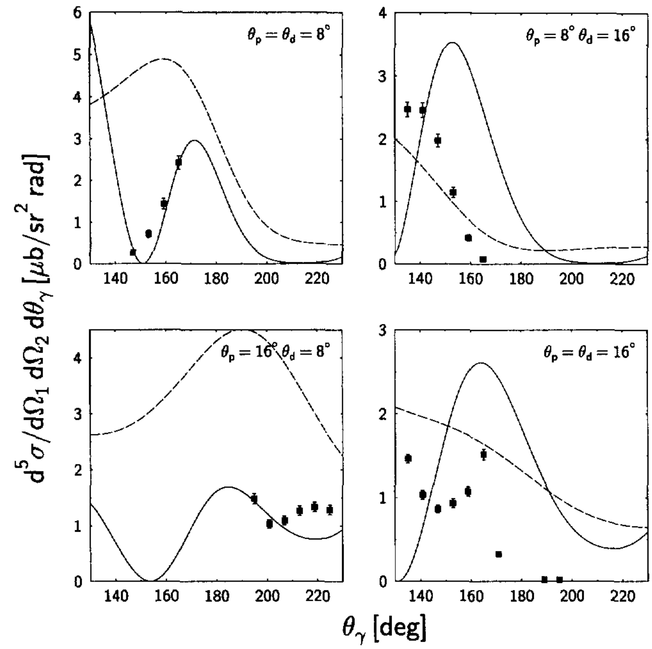

Figure 10. Preliminary *cross sections for the "coherent" proton-deuteron bremsstrahlung as a function of θ_γ for four different angle combinations (given in the figures). The dashed curve is an SPA calculation for the pn system downscaled by a factor of 3 and the solid line is a classical calculation (with an arbitrary normalization) for the pd system.*

no momentum, and only the protons took part in the bremsstrahlung process (4-body final state). The Fermi motion of the protons will affect the kinematics considerably. However, the largest part of the cross section comes from the low-momentum part of the wave function. Figure 12 illustrates the cross sections for different angle combinations as a function of the outgoing photon angle. The calculations shown in the figure are identical to the free proton-proton bremsstrahlung case. The differences must then be allocated to final-state effects and the effect of the folding, in the calculations, of the deuteron wave function.

6. SUMMARY AND OUTLOOK

In this contribution, the most complete bremsstrahlung measurements on $p+p$ and $p+d$ systems have been outlined. All the measurements were done with the new superconducting cyclotron, AGOR, at KVI with a (polarized) proton beam with an energy of 190 MeV. The detection systems SALAD (specially built for these measurements) and TAPS were utilized for these investigations. A hole in the center of all detection systems allowed us to measure the outgoing particles at very small angles enlarging the energy of the bremsstrahlung photons detected in coincidence. For the first time, liquid targets

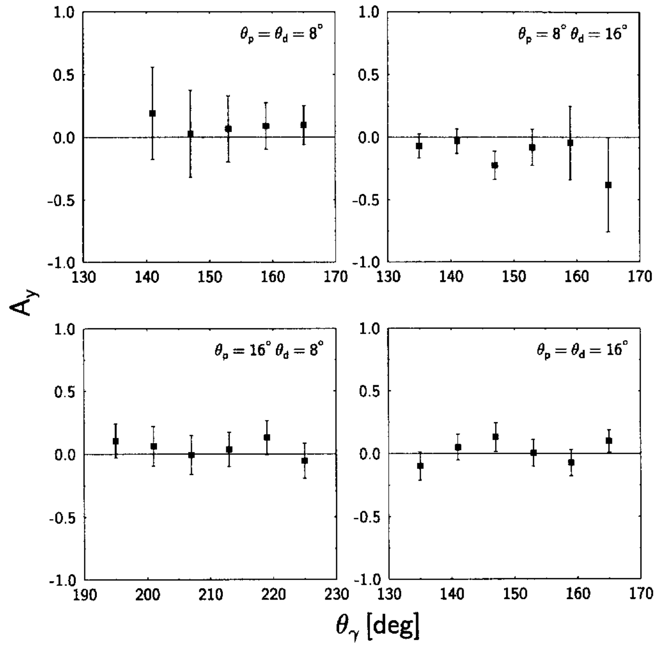

Figure 11. Preliminary *analyzing powers of the "coherent" proton-deuteron bremsstrahlung for the same combinations as in the last figure. No calculations are performed for this observable.*

contained within very thin foils were used for these systems eliminating the need for a good target-window study. Since most of the outgoing channels of these reactions are kinematically overdetermined, the background levels were reduced to a minimum allowing the extraction of cross sections and analyzing powers which are extremely clean. The elastic cross sections on both systems serve as a monitor of the integrity of the system and as a luminosity monitor.

In the case of the free $p+p$ system, very high-accuracy cross sections are obtained for the real-photon production which, apart from absolute normalization, do not agree with the most recent calculations which attempt to include all the possible effects, except Coulomb corrections which should be negligible for the kinematics considered here. The only parameter which can still be varied is the magnetic transition moment between positive- and negative-energy states. Chiral Perturbation Theory puts no bound on this parameter allowing one to look at differences in observables as a function of this "variable" [50]. There is still a large part of the phase space which has been measured and should be analyzed. Data with high statistical accuracies from non-coplanar geometries will be looked at which will certainly produce interesting physics and new observables, never measured before. For the first time, we have also done exclusive measurements of virtual-photon production on light systems.

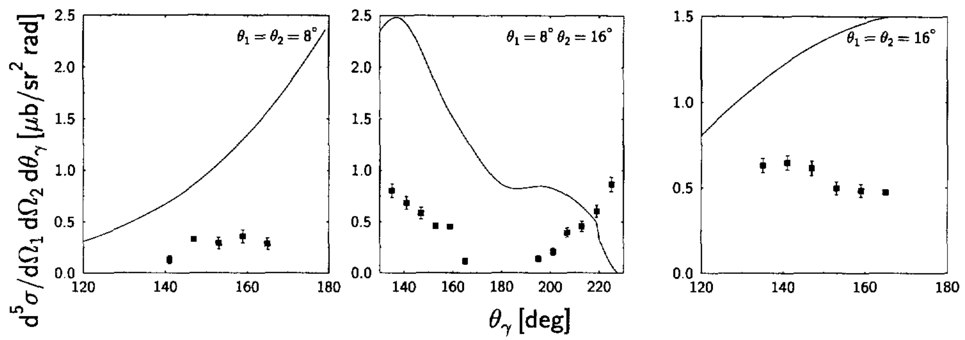

Figure 12. Preliminary *cross sections for the "quasi-free" proton-proton bremsstrahlung of the pd system. The calculation is the same as that for the free pp bremsstrahlung.*

For the $p+d$ system, different outgoing channels were investigated. In the first phase of the experiment, reported here, no neutron detection was yet possible. The radiative-capture channel was energetically separated. In the present experiment, we only looked at the photons with the highest energy and extracted cross sections and analyzing powers which agree reasonably well with the earlier results. The "coherent" proton-deuteron bremsstrahlung was also measured and, for the first time, cross sections and analyzing powers were obtained. No reliable calculation exists for this channel. To look at the effect of folding of the wave function, the "quasi-free" proton-proton bremsstrahlung from the $p+d$ reaction was studied. The cross sections obtained for this reaction were compared to the free proton-proton bremsstrahlung cross sections and the big difference between them demonstrates the need for the inclusion of the final-state effects and the initial-state wave function.

Very recently, after the completion of the proton-proton bremsstrahlung measurements which required high counting rates, SALAD was modified to detect neutrons as well, at the cost of lowering the total count rate that can be handled. The experiment, just completed, will open the way to investigate the angular distribution of the cross section and the analyzing power for all possible channels in the $p+d$ system for the first time, simultaneously.

7. ACKNOWLEDGEMENT

I would like to acknowledge the assistance of all those who helped build and commission SALAD, took part in all the preparations and data taking and are involved in the analysis. The enthusiasm and willingness of the AGOR (accelerator) group at KVI is most appreciated. The mechanical and electrical groups at KVI were involved in every aspect of the design and building of the detector. F. Mul and his group from Amsterdam were instrumental in shaping the final design of the scintillator part and the housing of SALAD. K. Solberg and his group at IUCF were the ones who helped me realize the idea of wire chambers with the hole in the center. The assistance of J. Mulder and J.

Zijlstra was extremely essential for the construction of the target system. The help of the TAPS collaboration in bringing TAPS to KVI is acknowledged. Last, I like to thank J.C.S. Bacelar, A. Bakker, M.J. van Goethem, M.N. Harakeh, M. Hoefman, A. Kugler, H. Löhner, R.W. Ostendorf, R. Simon, R. Turrisi, V. Wagner, H.W. Wilschut for their contributions during the different phases of the experiment and in particular, H. Huisman, J.G. Messchendorp, M. Volkerts and S. Schadmand who have done the analysis of the work presented here. The discussions with the theorists at KVI, O. Scholten, R. Timmermans, A.Yu. Korchin, G. Martinus and S. Kondratyuk were valuable and I should also thank them for providing all the calculations for our kinematics.

REFERENCES

1. J. Ashkin and R.E. Marshak, Phys. Rev. 76 (1949) 58, ibid. 76 (1949) 989.
2. F.E. Low, Phys. Rev. 110 (1958) 974.
3. H. Feshbach and D.R. Yennie, Nucl. Phys. 37 (1962) 150.
4. M.I. Sobel and A.H. Cromer, Phys. Rev. 132 (1963) 2698.
5. See D. Drechsel and L.C. Maximon, Ann. Phys. (N.Y.) 49 (1968) 403 for a clear discussion on the kinematics of the bremsstrahlung problem.
6. V.R. Brown, Phys. Lett. 25B (1967) 506; Phys. Rev. 177 (1969) 1498.
7. M.K. Liou and M.I. Sobel, Ann. Phys. (N.Y.) 72 (1972) 323.
8. See D. Marker and P. Signell, Phys. Rev. 185 (1969) 1286 for a comparison between different model calculations by different authors.
9. B. Gottschalk, W.J. Shlaer and K.H. Wang, Nucl. Phys. A94 (1967) 491; Nucl. Phys. 75 (1966) 549.
10. K.W. Rothe, P.F.M. Koehler, and E.H. Thorndike, Phys. Rev. 157 (1967) 1247.
11. Summary of the Contributions of the "Workshop on NN Bremsstrahlung and Polarization Observables", Groningen, 16-18 November, 1992.
12. K. Michaelian, P. Kitching, D.A. Hutcheon, R. Abegg, G.H. Coombes, W.K. Dawson, H.W. Fearing, H. Fielding, G. Gaillard, P. Green, L.G. Greeniaus, M. Hugi, C.A. Miller, G.C. Neilson, W.C. Olsen, J. Soukup, N.R. Stevenson, J. Wesick, and R.L. Workman, Phys. Rev. D41, (1990) 2689.
13. B. von Przewoski, H.O. Meyer, H. Nann, P.V. Pancella, S.F. Pate, R.E. Pollock, T. Rinckel, M.A. Ross, and F. Sperisen, Phys. Rev. C45 (1992) 2001.
14. H.W. Fearing, Nucl. Phys. A463 (1987) 95c.
15. V. Herrmann, J. Speth, and K. Nakayama, Phys. Rev. C43 (1991) 394.
16. V.R. Brown, P.L. Anthony, and J. Franklin, Phys. Rev. C44 (1991) 1296.
17. A. Katsogiannis and K. Amos, Phys. Rev. C47 (1993) 1376.
18. M. Jetter, H. Freitag, and H.V. von Geramb, Phys. Scr. 48 (1993) 229.
19. J.A. Eden and M.F. Gari, Phys. Lett. B347 (1995) 187; Phys. Rev. C53 (1996) 1102.
20. V. Herrmann and K. Nakayama, Phys. Rev. C45 (1992) 1450.
21. H.W.L. Naus and J.H. Koch, Phys. Rev. C36 (1987) 2459.
22. P.C. Tiemeijer and J.A. Tjon, Phys. Rev. C42 (1990) 599.
23. J.W. Bos and J.H. Koch, Nucl. Phys. A563 (1993) 539.
24. V. Herrmann and K. Nakayama, Phys. Rev. C44 (1991) R1254.
25. V. Herrmann, K. Nakayama, O. Scholten, H. Arellano, Nucl. Phys. A582 (1995) 568.

26. F. de Jong, K. Nakayama, V. Herrmann, O. Scholten, Phys. Lett. B333 (1994) 1; F. de Jong, K. Nakayama and T.-S. H. Lee, Phys. Rev. C51 (1995) 2334.
27. M. Jetter and H.W. Fearing, Phys. Rev. C51 (1995) 1666.
28. C. Dupont, C. Déom, P. Leleux, P. Lipnik, P. Macq, A. Ninane, J. Pestieau, S.W. Kitwanga and P. Wauters, Nucl. Phys. A481 (1988) 424.
29. F. Malek, H. Nifenecker, J.A. Pinston, F. Schussler, S. Drissi and J. Julien, Phys. Lett. B266 (1991) 255.
30. J.L. Matthews, Slide report of the "Workshop on Nucleon-Nucleon Bremsstrahlung", Groningen, 21 July, 1997.
31. J.A. Pinston, D. Barneoud, V. Bellini, S. Drissi, J. Guillot, J. Julien, H. Nifenecker and F. Schlussler, Phys. Lett. B249 (1990) 402.
32. J. Clayton, W. Benenson, M. Cronqvist, R. Fox, D. Krofcheck, R. Pfaff, T. Reposeur, J.D. Stevenson, J.S. Winfield, B. Young, M.F. Mohar, C. Bloch and D.E. Fields, Phys. Rev. C45 (1992) 1810.
33. J.-M. Laget, Phys. Rev. C38 (1989) 2993; S. Nagorny, private communication.
34. K. Nakayama, Phys. Rev. C45 (1992) 2039.
35. O. Scholten, private communication.
36. A.Yu. Korchin and O. Scholten, Nucl. Phys. A581 (1995) 493; A.Yu. Korchin, O. Scholten and D. Van Neck, Nucl. Phys. A602 (1996) 423.
37. M. Volkerts, A. Bakker, N. Kalantar-Nayestanaki, H. Fraiquin, A. Eads, T. Rinckel and K. Solberg, to be submitted to Nucl. Inst. and Meth.
38. S. Schadmand, J.C.S. Bacelar, H. van der Duin, N. Kalantar-Nayestanaki and H.W. Wilschut, to be submitted to Nucl. Inst. and Meth.
39. O. Schwalb, G. Enders, K. Hagel, W. Kühn, V. Metag, R. Novotny, W. Arnold, U. Kneissl, F. Steiper and T. Weber, Nucl. Inst. and Meth. A295 (1990) 191; H. Ströher, Nucl. Phys. News Int. Vol. 6, No. 1 (1996) 7.
40. J.G. Messchendorp et al., these proceedings.
41. N. Kalantar-Nayestanaki, J. Mulder and J. Zijlstra, to be submitted to Nucl. Inst. and Meth.
42. H. Witała, private communication.
43. M.K. Liou, R. Timmermans, B.F. Gibson, Phys. Lett. B345 (1995) 372; Phys. Rev. C54 (1996) 1574.
44. R. Timmermans, private communication.
45. G. Martinus, O. Scholten and J. Tjon, Phys. Lett. B402 (1997) 7; Phys. Rev. C, in press.
46. J.G. Rogers, J.L. Beveridge, D.P. Gurd, H.W. Fearing, A.N. Anderson, J.M. Cameron, L.G. Greeniaus, C.A. Goulding, C.A. Smith, A.W. Stetz, J.R. Richardson and R. Frascaria, Phys. Rev. C22 (1980) 2512.
47. V. Herrmann and K. Nakayama, Phys. Lett. B251 (1990) 6.
48. A. Katsogiannis, K. Amos, M. Jetter and H.V. von Geramb, Phys. Rev. C49 (1994) 2342.
49. M.A. Pickar, H.J. Karwowski, J.D. Brown, J.R. Hall, M. Hugi, R.E. Pollock, V.R. Cupps, M. Fatyga, and A.D. Bacher, Phys. Rev. C35 (1987) 37.
50. S. Kondratyuk, G. Martinus, O. Scholten, Submitted to Phys. Lett.